Bridging the Macroscopic and Atomistic Descriptions of the Electrocaloric Effect

I. Ponomareva and S. Lisenkov

Phys. Rev. Lett. **108**, 167604 — Published 20 April 2012

DOI: 10.1103/PhysRevLett.108.167604

Bridging the macroscopic and atomistic descriptions of electrocaloric effect

I. Ponomareva* and S. Lisenkov

Department of Physics, University of South Florida, Tampa, Florida 33620, USA

Abstract

First-principles-based simulations are used to simulate the electrocaloric effect (ECE) in $Ba_{0.5}Sr_{0.5}TiO_3$ alloys. In analogy with experimental studies we simulate the effect directly and indirectly (via the use of Maxwell thermodynamics). Both direct and indirect simulations utilize the same atomistic framework that allows us to compare them in a systematic way and with an atomistic precision for the very first time. Such precise comparison allows us to provide a bridge between the atomistic and macroscopic descriptions of the the ECE and identify the factors that may critically compromise or even destroy their equivalence. Our computational data reveal the intrinsic features of ECE in ferroelectrics with multiple ferroelectric transitions and confirm the potential of these materials to exhibit giant electrocaloric response. The coexistence of negative and positive ECE in one material as well as an unusual field-driven transition between them is predicted, explained at an atomistic level, and proposed as a potential way to enhance the electrocaloric efficiency.

PACS numbers: 77.70.+a,77.80.-e,77.22.Ej,65.40.G-

Caloric effects, such as magnetocaloric and electrocaloric effects, have attracted a lot of attention recently in the context of increasing interest in energy conversion and renewable energy materials and devices [1, 2]. ECE, for example, is associated with a reversible change in temperature under the application or removal of an electric field under adiabatic conditions. Adiabatic conditions are required to conserve the total entropy which is the sum of configurational entropy associated with a dipoles' disorder and thermal (or vibrational) entropy associated with disorder in the dipoles' kinetic energies [3]. A positive/direct (negative/inverse) ECE application of an electric field leads to an increase (decrease) in temperature. Quantitatively, ECE is measured by the change in temperature, $\Delta T = T - T_0$, achieved by an application of the electric field $\Delta E = E - E_0$. Traditionally, there exists two approaches to obtain $\Delta T(\Delta E)$: *direct* and *indirect*. In the first one $\Delta T(\Delta E)$ is directly measured under adiabatic conditions. This approach, although extremely desirable, is also very challenging [4]. The indirect approach is based on the use of Maxwell thermodynamical relation:

$$\frac{dT}{dE_i} = -\frac{T}{C_E}\left(\frac{\partial D_i}{\partial T}\right)_{E_i}, \tag{1}$$

where D_i and E_i are the i^{th} components of the electric displacement field and the electric field, respectively. C_E is the heat capacity under constant electric field. Eq.(1) is a first-order differential equation with a solution $T(E)$ satisfying the initial condition $T(E_0) = T_0$. In all cases of practical interest, this equation cannot be solved analytically and is integrated numerically using experimental, theoretical or computational data for $\mathbf{D_E}(T)$ and C_E. The indirect approach is usually less demanding and, therefore, the dominant technique for estimating ECE and magnetocaloric effect. One may, however, wonder how well the macroscopic thermodynamic approach, which is at the heart of Maxwell relation, describes the ECE which derives its origin from the atomistic order-disorder interplay [3].

ECE is promising for solid state refrigeration technology and has been explored since 1960s [1]. However, the difficulty in developing this technology stems from the fact that only a very small change in temperature, usually 1-2 Kelvin at most, can be achieved via such effect. Recently, the interest in ECE was fueled by the reports of giant ECE in $PbTi_{0.05}Zr_{0.95}O_3$ thin films [5] and ferroelectric polymers [6]. The giant effects (of about 12 K) were predicted in the framework of indirect approach. Direct measurements reported both giant [7–9] and moderate [4, 10, 11] values. These makes us wonder if the giant ECE

occurs for a wide range of ferroelectric materials and if the indirect approach provides a reliable basis for caloric effect estimation. For example, Ref. 10 reported good agreement between the magnitude of ΔT obtained directly and indirectly in $BaTiO_3$, but qualitative differences were observed in the behavior of $\Delta T(T)$. Another recent work [9] focused on ferroelectric polymers and compared their directly measured ΔT with that extrapolated from the indirect measurement of Ref.6. They found that both predictions agree well for the two temperatures considered. At the same time the Maxwell equation failed to reproduce the direct measurements in relaxors [7] confirming the earlier theoretical predictions of inapplicability of Maxwell relations to study nonergodic systems with irreversibility [12]. The aforementioned questions are of ultimate importance since the expectations of giant ECE in ferroelectrics are the driving force behind the increasing scientific and technological efforts in this direction [1, 2].

In this Letter, we develop and use accurate first-principles-based simulations to answer these important questions from an atomistic point of view. In particular, we develop a computational technique that allows both direct and indirect simulations of ECE within the *same* atomistic framework. We then use this tool to provide a first systematic comparison between ECE estimates obtained from both direct and indirect approaches which will allow us to bridge the macroscopic and atomistic descriptions of ECE. The results of our direct atomistic simulations are then used to explore the intrinsic features of ECE in ferroelectrics with multiple transitions.

We simulate $Ba_{0.5}Sr_{0.5}TiO_3$ disordered alloy since it exhibits a rich variety of ferroelectric transitions and was predicted to have good electrocaloric properties near the room temperature [3]. This material undergoes three ferroelectric transitions: paraelectric cubic to ferroelectric tetragonal at $T_C = 250$ K with a preferred polarization direction along <100>, ferroelectric tetragonal to ferroelectric orthorhombic at $T = 180$ K with a preferred polarization direction along <110>, and orthorhombic to rhombohedral at T =140 K with a preferred polarization direction along <111> [13]. The bulk sample of this material was modeled by a 16x16x16 simulation supercell (20480 particles) periodic along three Cartesian directions and with Ba, Sr atoms distributed randomly among individual unit cells. x-, y-, and z-axes were chosen along [100], [010], and [001] crystallographic directions, respectively. The potential energy of the sample U^{pot} is given by the first-principles-based effective Hamiltonian of Ref.14 which is defined in terms of the following degrees of freedom: local mode

vectors (proportional to the local dipole moments in the sample's unit cells), inhomogeneous and homogeneous strain variables (that describe the local deformations of the unit cells). This Hamiltonian reproduces accurately the experimental composition-temperature phase diagram of disordered $Ba_xSr_{1-x}TiO_3$ solid solution [14], dynamical properties of $BaTiO_3$ [15], provide accurate predictions for $BaTiO_3/SrTiO_3$ superlattices [16] and have been used recently to study a variety of properties of $Ba_xSr_{1-x}TiO_3$ alloys [3, 17, 18]. For all simulations below the Curie point the sample is in a monodomain state.

To model the electrocaloric response of this sample in the framework of the indirect approach we follow a procedure which closely simulates the experimental route [19, 20], namely, we slowly cool the sample in the presence of an applied *dc* electric field E. Technically, for a given field E in the range of 0-1000 kV/cm the sample is annealed from $T = 450$ K down to $T = 5$ K in steps of 5 K. We use $3{\times}10^5$ sweeps of the Metropolis Monte Carlo (MC) algorithm [21] to equilibrate the sample at desired T and E. The equilibrium values of polarization is then calculated for each temperature and plotted in Fig.1(a). The electric field modifies the character of phase transition from first-order-like to a highly diffused and also shifts the Curie point up. The polarization curves were fitted with up to 8th degree polynomial which was used to calculate the pyroelectric coefficients $(\partial P_i/\partial T)_{E_i}$ [29]. Note that, for strongly polar materials, such as ferroelectrics, $D \sim P$ [19], and the derivative $(\partial D_i/\partial T)_{E_i}$ in Eq.(1) can be replaced with $(\partial P_i/\partial T)_{E_i}$. The heat capacity at a given field E was calculated from the internal energy of the unit cell as: $C_E = (\frac{\partial U_E^{pot}}{\partial T} + \frac{15}{2}k_B)/V$. Here U_E^{pot} is the potential energy at a given electric field E, k_B is the Boltzmann constant, V is the volume of the unit cell. Factor, $\frac{15}{2}$, reflects the fact that there are five atoms in the unit cell. U_E^{pot} as a function of temperature was obtained from our MC computations. At zero field our computed heat capacity $C_{E=0} = C_P =$2.58 MJ/Km^3 agrees well with the experimentally reported heat capacity $C_P =$2.53 MJ/Km^3 obtained at constant pressure P in barium titanate-based ceramics [22] [30]. The computational values of heat capacities and pyroelectric coefficients were used in Eq.(1) to calculate dT/dE. These data are shown by lines in Fig.1(b) and constitute the prediction from our indirect approach.

Next we turn to a direct approach to compute dT/dE as a function of the electric field and temperature. To derive our approach for direct ECE simulation, we start with the enthalpic form of the first law of thermodynamics: $d\mathcal{H} = dQ - x_i dX_i - D_i dE_i$, where $\mathcal{H} = U - X_i x_i - E_i D_i$ is the enthalpy. Here dQ is an infinitesimal quantity of heat, U is

the internal energy, X_i and x_i are the stress and strain, respectively. Since the caloric effect of interest is an adiabatic process ($dQ = 0$) that occurs under slowly varying electric fields ($E \approx const$) and constant stresses/pressure ($dX_i = 0$), it can be considered as an isoenthalpic process $\mathcal{H} = const$. To simulate this process we follow the spirit of microcanonical MC simulations [23] and introduce extra degrees of freedom, called "demons" (analogous to the conjugate momenta in the microcanonical formulations), that absorb/carry/redistribute energy to achieve $\mathcal{H} = const$ simulations. In our simulations $\mathcal{H} = (U^{pot} + \sum_{i=1}^{n_{dem}} E_i^{dem} - VX_ix_i - Z^*\mathbf{E}\sum_j \mathbf{u}_j)/V = H + \sum_{i=1}^{n_{dem}} E_i^{dem}$, where U^{pot} is the potential energy given by the effective Hamiltonian [14], E_i^{dem} is the energy carried by the i^{th} demon, Z^* is the Born effective charge, $\mathbf{u}_j$ is the local mode at the site j. H is the enthalpy less the energy of all demons. We include $n_{dem} = integer[(C_{E=0} - \partial U^{pot}/\partial T)/k_B] = 8$ demons per unit cell to correctly reproduce the computational $C_{E=0}$. At each isoenthalpic MC step an update for a degree of freedom is attempted and compared with the energy of a randomly (or sequentially) picked demon E_i^{dem}. If $E_i^{dem} - \Delta H > 0$ the move is accepted and $H \to H + \Delta H$ and $E_i^{dem} \to E_i^{dem} - \Delta H$. One MC sweep attempts to update all the degrees of freedom sequentially. The temperature is calculated after each sweep as $T = \sum_{i=1}^{n_{dem}} E_i^{dem}/k_B n_{dem}$ and is typically averaged over 20,000 sweeps.

In our direct approach we first equilibrate the sample at the desired temperature T_0 using 3×10^5 MC sweeps of Metropolis algorithm. We next switch to $\mathcal{H} = const$ simulations and slowly increase the electric field from 0 up to 1000 kV/cm at a rate of 0.001 kV/cm per one MC sweep. The temperature T at a given field E is calculated from the average demon energy obtained at the same field. The associated temperature changes $\Delta T = T - T_0$ for some T_0 are given in the inset to Fig.2. The dependencies $\Delta T(\Delta E)$ were fitted with up to 5th degree polynomials which were used to calculate the derivatives dT/dE. The data points from these calculations are shown in symbols in Fig.1(b). This figure indicates a remarkable agreement between the data for the electrocaloric response dT/dE obtained from the direct and indirect approach for all investigated temperatures and electric fields. It further reveals the strong dependence of dT/dE on both the electric field and the temperature. One important consequence of this strong dependence is that a very fine mesh of points $P_i(T_i, E_i)$ is required to accurately integrate Eq.(1), especially at lower fields. Another important consequence is that for some materials (that are similar to the ones studied here) the approximation $\Delta T = -\int_{E_0}^{E_0+\Delta E} \frac{T}{C_E}\left(\frac{\partial D_i}{\partial T}\right)_{E_i} dE$ is likely to be crude and,

therefore, accurate numerical integration techniques should be used instead. We, therefore, conclude that the indirect approach based on Maxwell relation provides an accurate and reliable basis for electrocaloric response computations as long as the differential equation is properly integrated. This conclusion can be further generalized into the equivalence of macroscopic and atomistic descriptions of the ECE for the quantitative estimates of electrocaloric ΔT.

Next we will focus on the predictions of ΔT from our direct approach given in Fig.2. Note that the electric field was applied along the polarization direction. Firstly, we observe that indeed a giant electrocaloric response of 12 K can be obtained in ferroelectrics under sufficiently large fields as was predicted from recent experiments [5, 6]. Our data further indicate that ΔT peaks near the transition temperatures which is the consequence of the larger configurational disorder associated with these points and is in agreement with previous reports [24–27]. For a given ΔE, ΔT is always maximized near the Curie point T_C. For larger fields with ΔE applied above T_C, ΔT shows considerably less dependence on T_0 as compared with the data obtained for smaller fields. For instance, for $\Delta E \geq 500$ kV/cm the alloy exhibits good electrocaloric properties in a wide range of temperatures above T_C. This is a consequence of the diffused character of the phase transition under large electric fields. This feature is desirable for solid-state refrigeration which relies on good caloric response in a wide temperature range. All our findings are in good qualitative agreement with experimental data obtained for $Pb(Mg_{1/3}Nb_{2/3})O_3$-$PbTiO_3$ single crystals [24, 28]. Note, that a quantitative comparison is not possible since different materials and electric fields have been used.

Interestingly, one striking feature differentiates between our first-principles-based data and experimental findings of Ref.24. We do not find the negative electrocaloric response that was reported for some temperatures in the ferroelectric phase of <011>-oriented $Pb(Mg_{1/3}Nb_{2/3})O_3$-$PbTiO_3$ single crystals [24]. Our atomistic simulations reveal that this negative effect originates from noncollinearity between polarization and electric field. Indeed, if an electric field is applied along the polarization direction, it orders the dipoles, thus decreasing the configurational entropy. This leads to an increase in the temperature and positive ECE. If, however, a field is applied in the direction different from the polarization direction, it creates disorder since some of the dipoles flip to align with the electric field. As a result, the configuration entropy will increase causing the temperature to drop

(negative ECE). Indeed, Fig.2 confirms that if the electric field is applied along the polarization direction then ΔT is always positive. To introduce an angle between the electric field and polarization we apply a field along the [001] direction and repeat all simulations. The angle between this field and the polarization is 0° in the tetragonal phase, 45.0° in the orthorhombic phase, and 54.7° in the rhombohedral phase. To fully understand the effect of noncollinear electric field on the ECE we start by analyzing how this field influences the ferroelectric phases and the transition temperatures. We found that noncollinear electric field may; 1) induce transition between different ferroelectric phases; 2) lead to formation of low-symmetry monoclinic phases and; 3) shift the transition temperatures. An example of this is given in Fig.3(a). We first notice that for the temperatures below 155 K the noncollinear electric field induces monoclinic phases which are associated with positive derivatives $\partial P_z/\partial T$ in the temperature region of 90-155 K. This positive derivatives give rise to negative ECE (see Fig.3(b) for an example) in accordance with Eq.(1). Moreover, the comparison of our data for collinear and noncollinear fields (see Fig.3(b) for an example) reveals that the sign of ECE is controlled by the electric field's direction. Secondly, Fig.3(a) indicates that the transition from ferroelectric tetragonal phase to ferroelectric orthorhombic phase occurs at temperature 155 K which is 25 K below the same transition temperature in the absence of the electric field. This is a consequence of a field-induced transition from orthorhombic to tetragonal phase [31] that occurs for the temperatures in between 155 K and 180 K when an electric field of 300 kV/cm is applied. Interestingly, at the point of this transition, the polarization rotates towards the electric field which reduces configurational entropy and results in a sign change for ECE going from negative to positive (see Fig.3(b), solid circles). The latter is in excellent qualitative agreement with the recent experimental findings [24]. We, therefore, conclude that the sign of ECE can be efficiently controlled by the direction of applied electric field. This could open new ways to enhance electrocaloric efficiency by combining positive and negative ECE in one refrigeration cycle (see inset to Fig.3(b), for example).

In summary, we have employed atomistic first-principles-based simulations to reveal that both direct and indirect approaches yield the same qualitative and quantitative predictions for the ECE. In practice, however, the accuracy of indirect approach is limited by the accuracy of numerical integration of the Maxwell differential equation(s). We have also reported the intrinsic features of the ECE in ferroelectrics with multiple transitions which

include the potential to exhibit giant electrocaloric response under large electric fields and the coexistence of both positive and negative ECE in one material. The origin of negative ECE is traced to the noncollinearity between the electric field and the polarization which could lead to new ways to enhance the electrocaloric efficiency.

Acknowledgments: The present work is supported by the U.S. Department of Energy, Office of Basic Energy Sciences, Division of Materials Sciences and Engineering under award DE-SC0005245 (computational studies) and by USF under Grant No. R070699 (some theoretical developments). The use of services provided by Research Computing, USF is greatly acknowledged.

---

* Electronic address: iponomar@usf.edu

[1] J. F. Scott, Ann. Rev. Mat. Sci. **41**, 229 (2011).

[2] S.-G. Lu and Q. Zhang, Advanced Materials **21**, 1983 (2009).

[3] S. Lisenkov and I. Ponomareva, Phys. Rev. B **80**, 140102 (2009).

[4] B. Rožič, B. Malič, H. Uršič, J. Holc, M. Kosec, B. Neese, Q. M. Zhang, and Z. Kutnjak, Ferroelectrics **405**, 26 (2010).

[5] A. Mischenko, Q. Zhang, J. Scott, R. Whatmore, and N. Mathur, Science **311**, 1270 (2006).

[6] B. Neese, B. Chu, S.-G. Lu, Y. Wang, E. Furman, and Q. Zhang, Science **321**, 821 (2008).

[7] S. G. Lu, B. RoziC, Q. M. Zhang, Z. Kutnjak, R. Pirc, M. Lin, X. Li, and L. Gorny, Appl. Phys. Lett. **97**, 202901 (2010).

[8] S. G. Lu, B. RoziC, Q. M. Zhang, Z. Kutnjak, X. Li, E. Furman, L. J. Gorny, M. Lin, B. MaliC, M. Kosec, et al., Appl. Phys. Lett. **97**, 162904 (2010).

[9] S. G. Lu, B. Rožič, Q. M. Zhang, Z. Kutnjak, and B. Neese, Appl. Phys. Lett. **98**, 122906 (2011).

[10] S. Kar-Narayan and N. D. Mathur, Journal of Physics D: Applied Physics **43**, 032002 (2010).

[11] Y. V. Sinyavsky and V. M. Brodyansky, Ferroelectrics **131**, 321 (1992).

[12] C. M. Soukoulis, K. Levin, and G. S. Grest, Phys. Rev. Lett. **48**, 1756 (1982).

[13] V. V. Lemanov, E. P. Smirnova, P. P. Syrnikov, and E. A. Tarakanov, Phys. Rev. B **54**, 3151 (1996).

[14] L. Walizer, S. Lisenkov, and L. Bellaiche, Phys. Rev. B **73**, 144105 (2006).

[15] I. Ponomareva, L. Bellaiche, T. Ostapchuk, J. Hlinka, and J. Petzelt, Phys. Rev. B **77**, 012102 (2008).

[16] S. Lisenkov and L. Bellaiche, Phys. Rev. B **76**, 020102 (2007).

[17] S. Lisenkov, I. Ponomareva, and L. Bellaiche, Phys. Rev. B **79**, 024101 (2009).

[18] N. Choudhury, L. Walizer, S. Lisenkov, and L. Bellaiche, Nature **470**, 513 (2011).

[19] B. Tuttle, Ph.D. thesis, University of Illinois (1981).

[20] B. A. Tuttle and D. A. Payne, Ferroelectrics **37**, 603 (1981).

[21] N. Metropolis, A. Rosenbluth, M. Rosenbluth, and A. Teller, J. Chem. Phys. **21**, 1087 (1953).

[22] Yi and He, Thermochimica Acta **419**, 135 (2004).

[23] M. Creutz, Phys. Rev. Lett. **50**, 1411 (1983).

[24] J. Peräntie, J. Hagberg, A. Uusimäki, and H. Jantunen, Phys. Rev. B **82**, 134119 (2010).

[25] R. Pirc, Z. Kutnjak, R. Blinc, and Q. M. Zhang, Appl. Phys. Lett. **98**, 021909 (2011).

[26] R. Pirc, Z. Kutnjak, R. Blinc, and Q. M. Zhang, Journal of Applied Physics **110**, 074113 (2011).

[27] B. Rožič, M. Kosec, H. Uršič, J. Holc, B. Malič, Q. M. Zhang, R. Blinc, R. Pirc, and Z. Kutnjak, Journal of Applied Physics **110**, 064118 (2011).

[28] M. Valant, L. J. Dunne, A.-K. Axelsson, N. M. Alford, G. Manos, J. Peräntie, J. Hagberg, H. Jantunen, and A. Dabkowski, Phys. Rev. B **81**, 214110 (2010).

[29] Assuming primarily displacive nature of the ferroelectric phase in $Ba_{0.5}Sr_{0.5}TiO_3$, the pyroelectricity derives its origin from the temperature dependent displacements of ions from their centro-symmetric positions.

[30] Our numerical calculations reveal that, for the range of electric fields investigated, the heat capacity depends only weakly on the electric field.

[31] Such phases have different symmetry and, therefore, atomistically are associated with different ionic displacement patterns.

FIG. 1: (color online). (a) The dependencies $P(T)$ for electric fields in the range 0-1000 kV/cm. (b) The dependencies of dT/dE on the temperature for electric fields 100-900 kV/cm (in 100 kV/cm increments). The electric field is applied along the polarization direction. The predictions from direct and indirect approaches are shown with symbols and lines, respectively. The arrows indicate the direction of the electric field increase.

FIG. 2: (color online). The electrocaloric temperature change $\Delta T = T - T_0$ as a function of initial temperature T_0 for some fields $\Delta E = E - E_0$ applied along the polarization direction. Here E_0 =0 kV/cm. Dashed lines indicate the computational zero-field transition temperatures. Inset: Dependencies $\Delta T(\Delta E)$ for some selected T_0.

FIG. 3: (color online). (a) Dependence of the average polarization's components $< P_x >$, $< P_y >$, and $< P_z >$ on the temperature under an electric field of 300 kV/cm applied along the [001] direction. (b) The dependencies $\Delta T(\Delta E)$ for two selected temperatures T_0. Diamonds (circles) indicate data obtained when the electric field is collinear (noncollinear) to the polarization. The inset shows an idealized refrigeration cycle that utilizes both positive and negative ECE. The cycle begins (step 1) with application (increase) of a collinear electric field $E_{||}$ which is followed by a heat exchange with a sink under constant $E_{||}$ (step 2). At step 3 $E_{||}$ is removed (decreased) adiabatically resulting in the drop of the temperature below T_0 via positive ECE. At step 4 a noncollinear field $E_{\angle}$ is applied (increased) producing an additional drop in the temperature via negative ECE. At step 5 the system returns to the original T_0 by absorbing the heat from the load. The cycle closes via adiabatic removal (decrease) of $E_{\angle}$ (step 6) followed by the heat exchange with the sink (step 7). The $\Delta T = T_4 - T_0$ of the double cycle exceeds that of a single cycle which utilizes either positive ECE ($\Delta T = T_3 - T_0$) or negative ECE ($\Delta T = T_4 - T_3$).

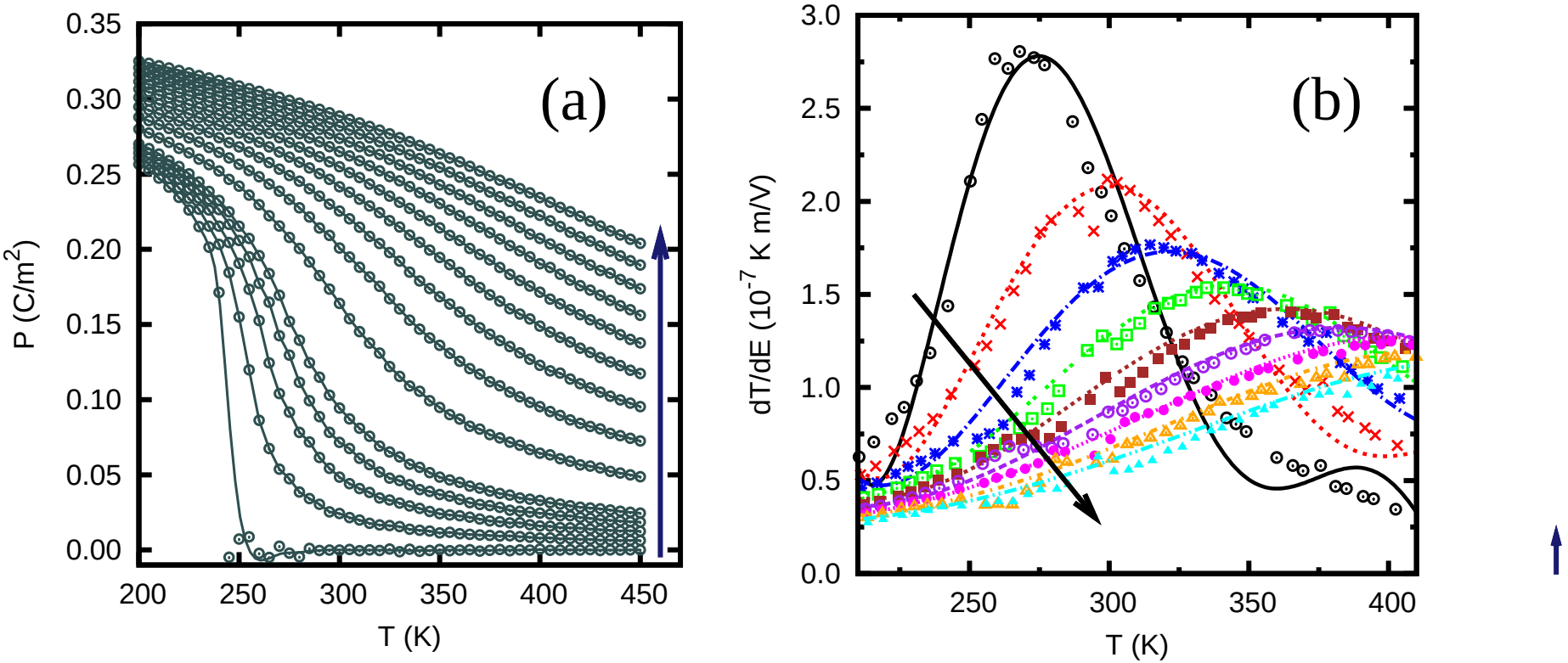

Figure 1 LK13234 15FEB12

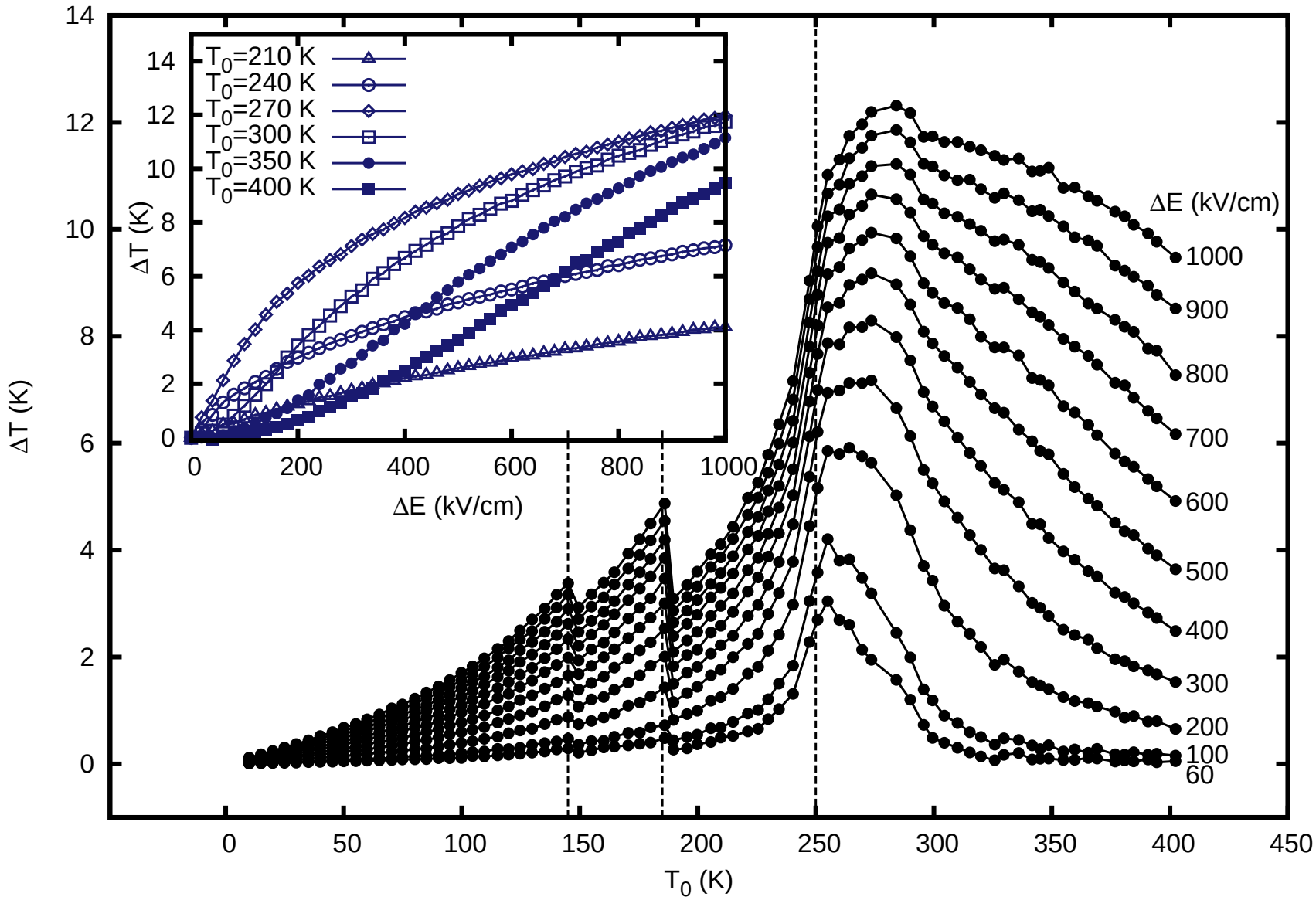

Figure 2 LK13234 15FEB12

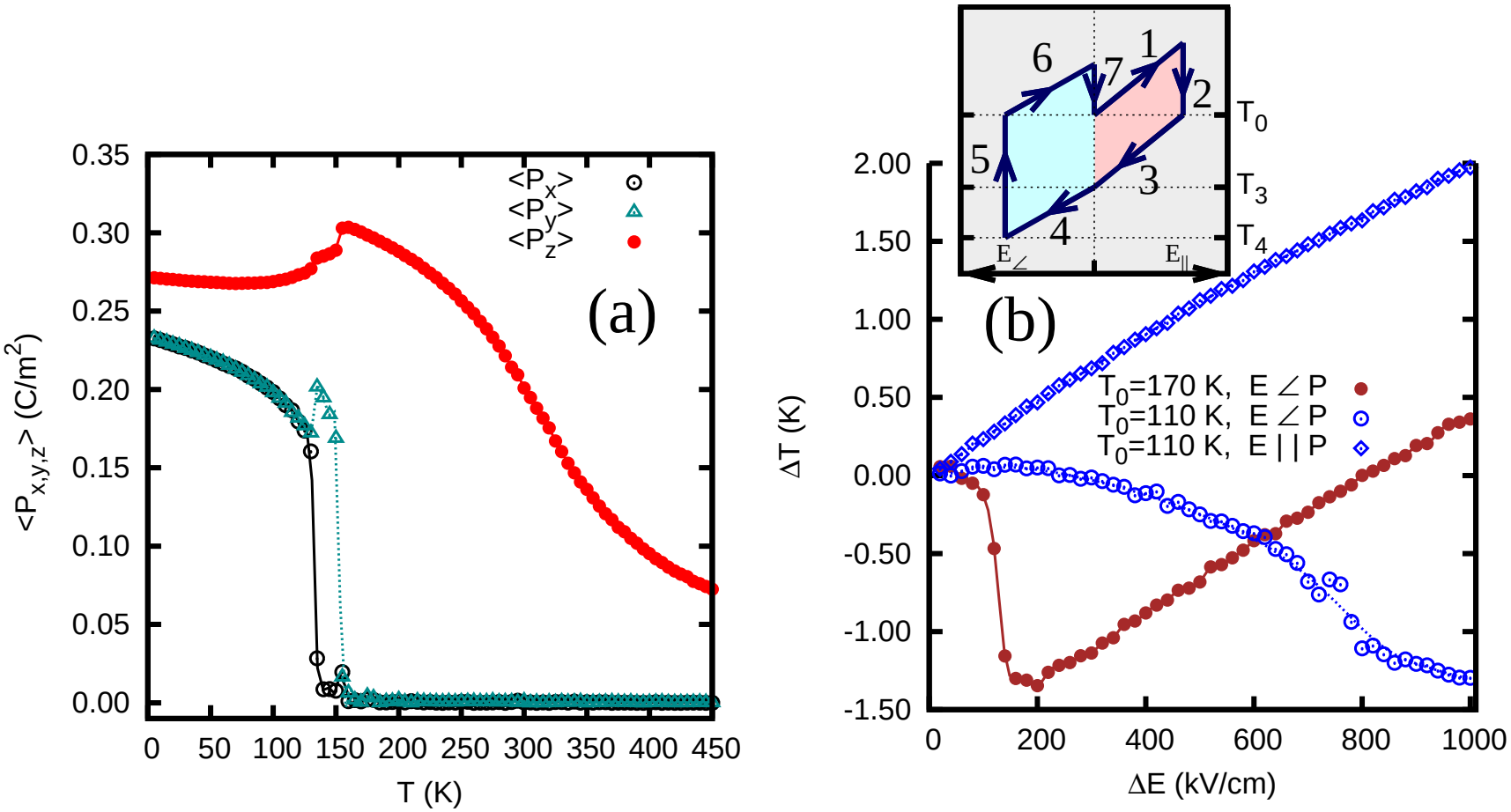

Figure 3 LK13234 15FEB12